Angular distribution of Ga^+ ions desorbed by 3-keV-ion bombardment of GaAs{001}-(2×4)

R. Blumenthal,* K. P. Caffey, E. Furman,† B. J. Garrison, and N. Winograd
Department of Chemistry, The Pennsylvania State University, 152 Davey Laboratory, University Park, Pennsylvania 16802
(Received 8 April 1991)

The angular distribution of Ga^+ ions desorbed from the molecular-beam-epitaxy-grown GaAs{001}-(2×4) surface by ion bombardment is presented. This distribution displays the highest degree of anisotropy, relative to the crystal direction of desorbed ions, which has been reported to date. The interpretation of the data is possible using physical arguments based on a simple geometric model of the desorption of ions from the surface. Further insight is provided by comparison to molecular-dynamics simulations of the keV-ion bombardment of metal and semiconductor surfaces. The experimental and calculated distributions of Ga^+ ions desorbed from the (2×4) surface are in reasonable qualitative agreement. The results indicate that the extreme anisotropy in the angular distribution results from a direct mechanism wherein a third-layer As atom collides with a second-layer Ga atom and thereby causes the Ga atom to eject along their mutual bond axis. This mechanism has been observed previously on Si and GaAs surfaces but is not commonly observed on metal surfaces, and can be ascribed to the directional bonding and open structure of covalent crystals. Other features of the angular distribution are related to blocking and channeling of the desorbed Ga^+ ions. These features indicate that there is one, and only one, missing row of As_2 dimers for every 16 Å unit-cell length along the 4× crystal direction. These results provide complementary information which is in excellent agreement with other studies of the GaAs{001}-(2×4) surface.

INTRODUCTION

The GaAs{001} surface structure is extraordinarily varied depending upon the surface coverage of Ga and As.[1] It is important to be able to characterize these structures in order to gain an atomistic picture of thin-film growth. Moreover, the GaAs{001} template is the one most widely used in the construction of microelectronic devices and has considerable technological relevance.[2] Until the development of scanning tunneling microscopy (STM), it had been virtually impossible to unravel the structure of these complex surfaces except by reflection high-energy electron diffraction (RHEED) (Ref. 1) and Auger electron spectroscopy (AES).[3] With the combination of these techniques and STM,[4,5] however, a general picture of the atomic ordering observed by RHEED is emerging. Detailed crystallographic information about this important surface is still astonishingly sparse.

The hypothetical unreconstructed GaAs{001} arsenic-terminated surface consists of a square array of As atoms bonded to two Ga atoms in the layer below, as shown schematically in Fig. 1. Each As atom possesses two partially filled "dangling bonds" pointing upwards and oriented parallel to the $\langle 0\bar{1}1 \rangle$ direction. The As atoms may pair up to form dimers along this direction, doubling the lattice periodicity, also shown in Fig. 1. In the laboratory, the (2×1) reconstruction is not observed. Instead, a series of RHEED patterns have been reported which range from an As-rich $c(4\times4)$ lattice to a Ga-rich (4×2) or $c(8\times2)$ lattice. The most important of these, with respect to crystalline thin films by molecular-beam epitaxy (MBE), is the As-rich (2×4) or $c(2\times8)$ structure, since growth usually begins and ends with this surface. Both of these reconstructions arise from the way in which As_2 dimers are arranged along the $\langle 011 \rangle$ direction. The STM observations have established that the

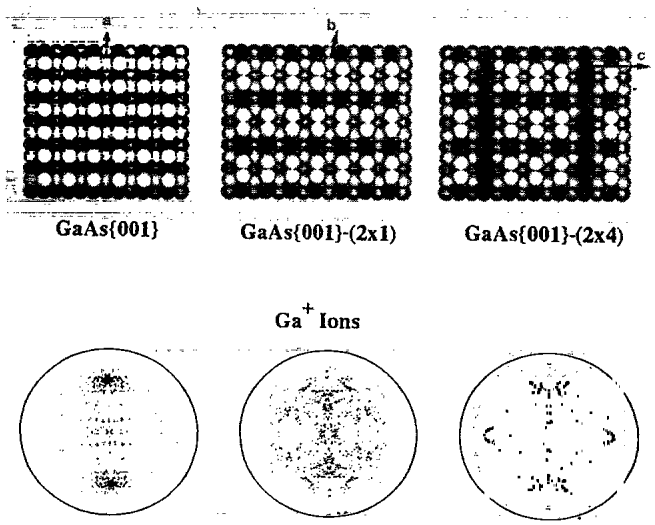

FIG. 1. Top panel: Representations of three hypothetical GaAs{001} surfaces. The white balls represent surface As atoms. The slightly shaded balls represent second-layer Ga atoms. Bottom panel: calculated angular distributions of 10–30-eV Ga^+ ions desorbed by keV Ar^+-ion bombardment of the corresponding GaAs{001} surface given in the top panel. The $\langle 011 \rangle$ azimuthal crystal direction is parallel to arrow (c) in the figure. The polar angle of Ga^+-ion emission is proportional to the distance of a spot from the center of the circle. Ion ejection mechanisms (a), (b), and (c) are discussed in the text.

periodicity along the ⟨011⟩ direction results from a regular array of missing As_2 dimers. A possible representation of the (2×4) reconstruction is shown in Fig. 1.

In connection with the characterization of GaAs single-crystal surfaces, we have been investigating the possibility of utilizing the angular distributions of Ga^+ ions desorbed from these surfaces to provide complementary structural information. These studies are potentially valuable since molecular-dynamics simulations of ion-induced desorption experiments have shown that the vast majority of detected atoms originate from the top three or four atomic layers.[6–8] In this context, the composition of the GaAs{001} surface, with alternating layers of exclusively As or Ga atoms, serves as a unique environment for the study of ion-induced desorption from semiconductor surfaces. The detection of one or the other species allows the experimental choice of probing the properties of atoms ejected from the first (As) layer or second (Ga) layer. Moreover, angular anisotropies are predicted to reflect the surface crystal structure, either through channeling and blocking of desorbing ions by other surface atoms or by direct collisions between atoms in the top three or four atomic layers, resulting in desorption along the direction of their common bond. In previous studies, for example, it has been possible to reconcile the chain rotation reconstruction associated with the GaAs{110} surface using this approach.[9]

In this paper, we examine the response of the MBE-grown GaAs{001}-(2×4) surface to 3-keV Ar^+-ion bombardment by measuring the angular distribution of desorbed Ga^+ ions. The results yield angular distributions with the highest degree of anisotropy reported to date. Moreover, the major features of the angular distributions are easily understandable from simple collision models without having to employ an extensive calculational effort.

EXPERIMENT

The experimental apparatus necessary to perform angle-resolved secondary-ion-mass-spectroscopy (SIMS) experiments on GaAs{001} surfaces is necessarily complex.[10] The MBE experiments are performed in a commercially available Riber 2300 growth chamber equipped with a 10-keV RHEED system for *in situ* monitoring of the growth conditions. After synthesis, the GaAs wafers are transferred under vacuum of less than 2×10^{-10} Torr through a sample introduction chamber into a surface analytical chamber. This chamber is equipped with a differentially pumped Leybold-Heraeus ion source and an Extrel C50 quadrupole mass spectrometer (QMS).

In the surface analytical chamber the detection angle may be altered independently by rotation of the differentially pumped QMS mounting flange. The QMS is equipped with a 90° electrostatic sector for energy selection. The input einzel lens has an acceptance aperture of 1.8 mm positioned 3.7 cm from the center of the experimental chamber. This results in a total polar angle acceptance of ±3° and a typical energy acceptance of 20±0.2 eV. The crystal manipulator allows independent translation along three Cartesian axes and independent rotation around two mutually perpendicular axes (parallel and perpendicular to the sample surface). Other details of this apparatus have been published elsewhere.[10] A schematic diagram of the configuration of the analysis chamber and the angle definitions are shown in Fig. 2.

The three angles can be determined with an accuracy better than ±1° and to a precision of ±0.1°. The total angular distribution is collected as a series of azimuthal angle scans at a fixed polar angle. Each scan is obtained by rotation of the sample in 1° steps over three full revolutions. The angle positions are set by computer-controlled stepping motors. For the data reported here, intensities of the various azimuthal scans, taken on different days, were normalized to a scan of the polar detection angle. Azimuthal scans are not corrected for the increase in azimuthal acceptance as the polar detection angle is decreased. This effect results in azimuthal acceptances of 3.3° and 1.5°, at polar angles of 25° and 70°, respectively.

Secondary-ion ejection is initiated by 4 nA, 3-keV Ar^+-ion bombardment at normal incidence. The ion beam is typically focused into a 2-mm spot which is incident on a >3-mm radius circle of the sample surface as it rotates through three full revolutions at each polar angle of ion detection. The total flux on the surface during a 20-min experiment is never greater than 3×10^{13} ions resulting in a maximum ion dose $<8\times10^{11}$ ions/mm^2. Data acquisition over three full revolutions of the sample provides an excellent internal monitor of bombardment-induced damage and any slippage in the rotational mechanism. Neither of these effects was observed in any of the scans obtained on the {001} surfaces as evidenced by a typical azimuthal distribution obtained at $\theta=42.5°$, shown in Fig. 3. We were only successful at detecting the Ga^+ ions under static conditions. The incident ion flux had to be increased to unacceptable levels to achieve any discernable As^-- or As^+-ion signal. This is not surprising since the SIMS analysis of GaAs crystals typically results in ion yields of As^+ and As^- that are two orders of magnitude below the ion yield of Ga^+.

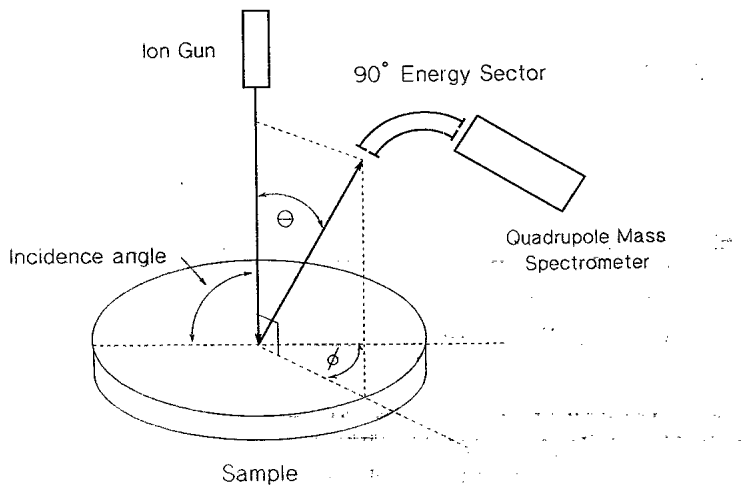

FIG. 2. A schematic of the angular definitions used in angle-resolved SIMS experiments. θ is the polar angle relative to the surface normal, and ϕ is the in-plane azimuthal angle.

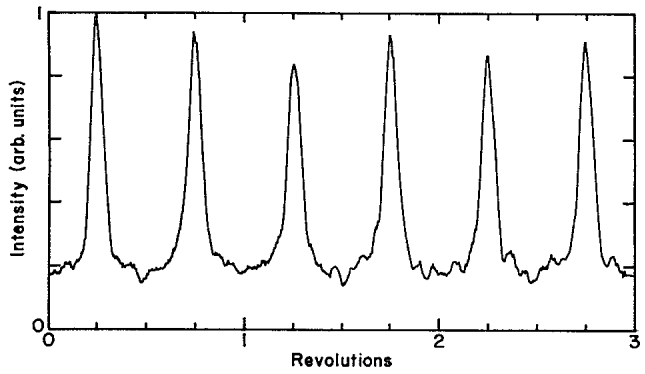

FIG. 3. The relative intensity of 20-eV Ga^+ ions desorbed from the GaAs{001}-(2×4) surface as a function of the azimuthal angle during three revolutions of the crystal. $\phi=0°$ corresponds to the ⟨011⟩ crystal direction, and the polar angle of detection is $\theta=42.5°$.

Semi-insulating Si-doped GaAs wafers were cut in the {001} plane obtained from M/A COM Laser Diodes, Inc. Prior to insertion into the UHV complex and initial MBE growth, each was degreased in 1,1,1-trichloroethane, acetone, and methanol followed by a water rinse and storage in sulfuric acid. The surface was then etched with a 5:1:1 H_2SO_4:H_2O_2:H_2O mixture. After decanting the etching solution, the samples were thoroughly rinsed with water, dried with nitrogen, and mounted on a molybdenum sample block with indium. Several samples were mounted directly and spin etched with a 5:1:1 solution, rinsed with water, and dried with nitrogen.

The GaAs films were grown at a substrate temperature of 580 °C under an 8:1 [As_4]:[Ga] flux ratio as measured by an ion gauge. Growth rates of ~1 μm/h were typically achieved as determined by intensity oscillations in the RHEED pattern[11] and film thickness measurements. Layers of at least 1 μm in thickness were deposited for each experiment. To insure that minor daily changes in the growth termination procedure did not result in the production of surfaces of differing composition, systematic growth termination procedures were developed for each surface reconstruction. The procedure developed for the preparation of a (2×4) reconstructed surface was as follows: the Ga flux was terminated with the sample still at growth temperature, the As flux was then reduced to $\frac{1}{20}$ of the growth flux by lowering the As oven temperature, and the sample was cooled to 350 °C. At this point the As flux was terminated, and the sample was cooled to less than 100 °C before sample transfer was initiated. This procedure allowed a sharp (2×4) RHEED pattern to be maintained throughout the entire process.

Once prepared, the wafers were transferred under UHV conditions to the surface analysis chamber within about 10 min for angle-resolved SIMS studies. As a test of surface order and any possible contamination that may be associated with transfer and analysis of samples, each sample was transferred back to the MBE chamber for RHEED characterization after a series of experiments was completed. Only data collected from wafers that exhibited no detectable degradation of the RHEED patterns were used for subsequent analysis.

RESULTS AND DISCUSSION

A schematic of the ideal GaAs{001}-(2×4) surface is presented in Fig. 4. The angular distribution of 20-eV Ga^+ ions desorbed from this surface by 3-keV Ar^+-ion bombardment is displayed in Figs. 5(a) and 5(b). A selected set of azimuthal scans is shown in Fig. 6. The distribution appears to be highly anisotropic and is dominated by two large peaks oriented in the ⟨01$\bar{1}$⟩ ($\phi=90°$) and ⟨0$\bar{1}$1⟩ ($\phi=270°$) directions. At polar angles of $\theta>45°$, shoulders appear on either side of the major peaks. These shoulders persist to the highest measured polar angles. Finally, at $\theta>60°$ the major peaks are no longer visible and two new peaks are seen near the ⟨011⟩ ($\phi=180°$) direction.

It is possible to assign each of the important features that appear in the angular distribution using the concepts developed to explain the Ga^+-ion distributions from bombarded GaAs{110}.[9] According to our hypothesis, the most intense peaks arise from atom-atom collisions between neighboring atoms, followed by desorption along the direction of their common bond. Since the mass spectrometer is set to monitor only the Ga^+-ion signal, these types of collisions can only arise between third-layer As atoms and second-layer Ga atoms as denoted by mechanism (a) in Fig. 1 or mechanism 1 in Fig. 4. Specifically, a third-layer As atom collides with a second-layer Ga atom and causes the Ga atom to eject along their mutual bond axis. Note that this type of mechanism would lead to ejection along $\phi=90°$ and $\phi=270°$ as observed. Moreover, the intensity would be expected to maximize near $\theta=54.7°$, the angle formed by the bulk As—Ga bond and the surface normal. The experimental value occurs at $\theta=45°$, as seen in Fig. 7. Although agreement with the predicted value is not very good, other factors such as blocking by the wall of As_2 dimers, surface relaxation, and image charge effects would tend to deflect the Ga^+ ions away from their straight-line trajectories.[9] The measurable intensity of $\theta<45°$ presumably results from the presence of more random collisions in the solid giving rise to an $\sim\cos^2\theta$ distribution, only possible along $\phi=90°$ and 270° because of blocking by the As overlayer atoms in other directions.

This direct ejection mechanism clearly dominates the distribution of ions ejected from GaAs{001} and other semiconductor surfaces. By comparison, this mechanism plays only a minor part in the angular distribution of ions (or neutrals) desorbed from metal surfaces, where ejection occurs in the most open direction of the crystal surface.[12–14] Specifically, a direct ejection mechanism has only been observed on the Rh{111} surface. It appears, through extensive theoretical study, that a 50% enhancement of ejection in one open direction of this surface, relative to another open direction, occurs as a result of a direct Rh-Rh collision along the bond direction.[14] The anisotropy of angular distributions of ions desorbed from semiconductor surfaces is much more pronounced, and the unique dominance of this ejection mechanism on

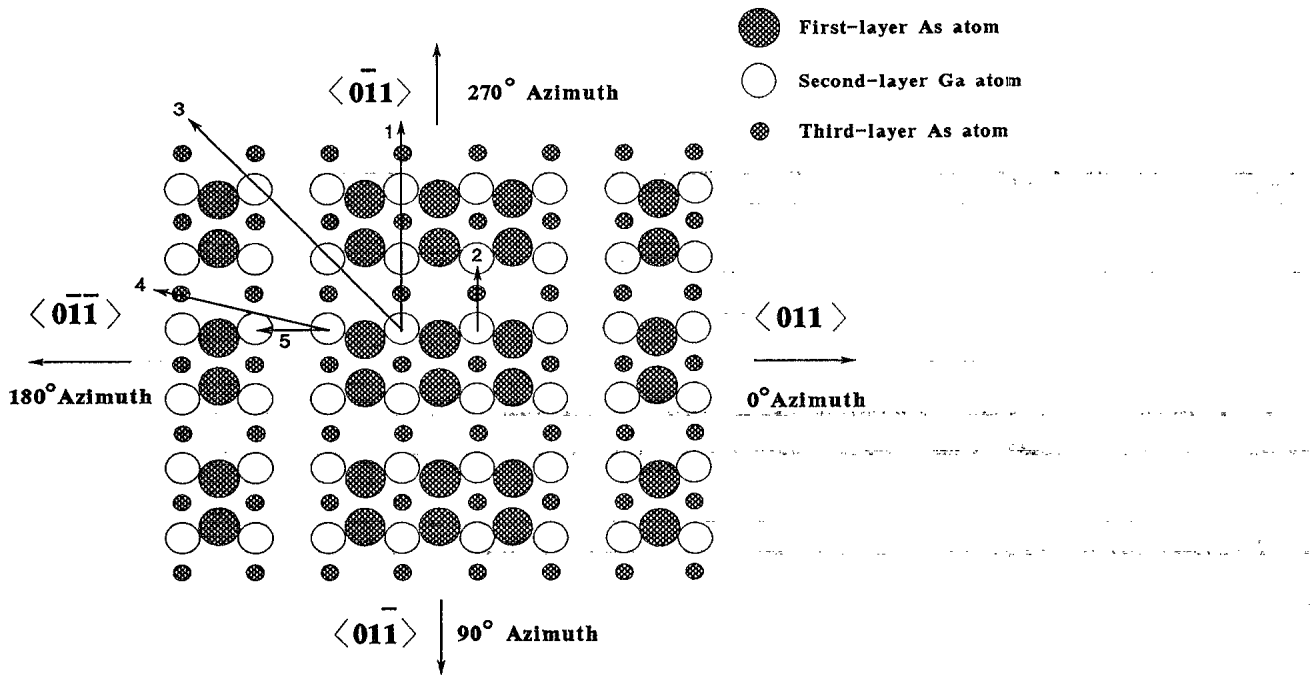

FIG. 4. A schematic of the GaAs{001}-(2×4) surface indicating mechanism directions 1–5, which are responsible for the spectral features of the secondary Ga^+-ion distributions shown in Figs. 5 and 6. Mechanism 1 is the direct ejection of Ga^+ ions by a collision event between the second-layer Ga atoms and third-layer As atoms along their mutual bond direction. Mechanism directions 2 and 5 indicate the blocking of desorbed secondary ions by surface As atoms, and mechanism directions 3 and 4 indicate the channeling of desorbed secondary ions by surface As atoms.

semiconductor surfaces has been attributed to the more open nature of these lattices.[7]

The second major feature in the Ga^+-ion distributions shown in Figs. 5 and 6 is related to the shoulders associated with the major peaks at $\phi=90°$ and 270°. These shoulders begin to appear at $\theta>45°$ and persist out to the highest measurable polar angle. The position of the peaks changes continuously with θ, reaching a limit of $\sim\pm40°$ on either side of the major peaks.

This mechanism is interesting because it appears at high polar angles in an azimuthal direction that is not associated with specific atom-atom collisions. Using channeling and blocking arguments, however, it is easy to assign its origin. As a result of the random portion of the collision cascade, a fraction of the Ga^+ ions will take off in all directions. Some of these will be blocked by surface As_2 dimers, or may be directed between the dimers. Many others will escape through the channel created by the missing dimers. This mechanism is illustrated by arrow 3 in Fig. 4. Note that as the polar angle of detection is increased, the repulsive wall of the As_2 dimers adjacent to the channel will deflect the escaping Ga^+ ions further away from the $\phi=90°$ and 270° directions as observed. A possible contribution to this channeled Ga^+ -ion signal may arise from atoms that are ejected by the previously described direct collisional mechanism, arrow 1 in Fig. 4, but which are subsequently deflected by the As_2 dimers adjacent to the channel. This mechanism occurs mainly for Ga atoms that are next to the channels, and the signal intensity would again peak in the direction of arrow 3 in Fig. 4. The presence of these peaks at polar angles $\theta>45°$ clearly indicates that there are open channels parallel to the ⟨0$\bar{1}$1⟩ direction of the GaAs{00$\bar{1}$}-(2×4) surface, caused by missing As_2 dimers. These two proposed mechanisms also have important implications for detecting additional atoms that may adsorb in the channel since these atoms would selectively attenuate this signal. We have in fact been able to identify the binding site of excess As atoms in this region within the framework of the (2×4) reconstruction by observing the decrease in intensity of these peaks at $\theta=55°$ as a function of As exposure, and also by observing the repositioning of these peaks at $\theta>55°$ as a function of As exposure.[15]

The peaks associated with mechanism 3 should exhibit mirror plane symmetry about $\phi=90°$ and 270°. As seen in Figs. 5 and 6, there are clearly deviations from the predicted symmetry. We are reluctant to place inordinate significance on this observation at the present time since it becomes a more challenging experimental problem to record precise azimuthal angle measurements at $\theta>60°$. We have observed this asymmetry repeatedly on samples cut from different boules and during clockwise and counterclockwise sample motion. However, the differences in intensity are presently sufficiently small that we are reluctant to interpret these data to mean, for example, that the As_2 dimers are slightly twisted.

The two large peaks seen at low polar angles, and at azimuthal angles of $\phi=90°$ and 270°, evolve into blocking features for polar angles of $\theta>55°$. At these high polar angles the ejection of Ga^+ ions, regardless of whether they originate from a direct collisional mechanism or a random portion of the collision cascade, is prevented in

the $\phi=90°$ and 270° directions by a repulsive wall of As_2 dimers, mechanism 2 in Fig. 4. This causes the signal intensity in these azimuthal directions to decrease from their peak value of >700 counts at $\theta=45°$ to <15 counts at $\theta=70°$. The azimuthal angular width of these blocking features is also very large, about 60° at high polar angles. The combination of extremely low intensity in the blocking minimum and large blocking feature width leads to the conclusion that very few, if any, Ga^+ ions have a clear ejection path in the $\phi=90°$ and 270° directions at high polar angles. This effectively excludes the possibility of more than one missing dimer per unit cell for the GaAs{001}-(2×4) surface. Any proposed structure with two or more missing dimers adjacent to each other would provide a clear ejection path for high-polar-angle Ga^+ ions, and conflict with the experimentally determined distributions. Similarly, a proposed structure of alternating missing dimers would result in a 2× periodicity along the ⟨011⟩ crystal direction instead of the 4× periodicity observed by RHEED.

The last important feature in the distribution are peaks seen, in Fig. 5(a), near $\phi=180°$ and at $\theta>55°$. These peaks cannot arise from any known atom-atom collision and are therefore probably explainable from surface channeling and blocking of Ga^+ ions ejected due to the random part of the collision cascade. A probable origin of these peaks is shown by mechanism (c) in Fig. 1 and mechanisms 4 and 5 of Fig. 4. In this case, the Ga^+ ions cannot eject at small values of θ since they are blocked by overlaying As atoms. At large values of θ, however, they can escape through the channel created by the missing As_2 dimers. The minimum at $\phi=180°$ is probably due to blocking by an As_2 dimer across the row as illustrated in Fig. 4.

The simple arguments presented above provide a satis-

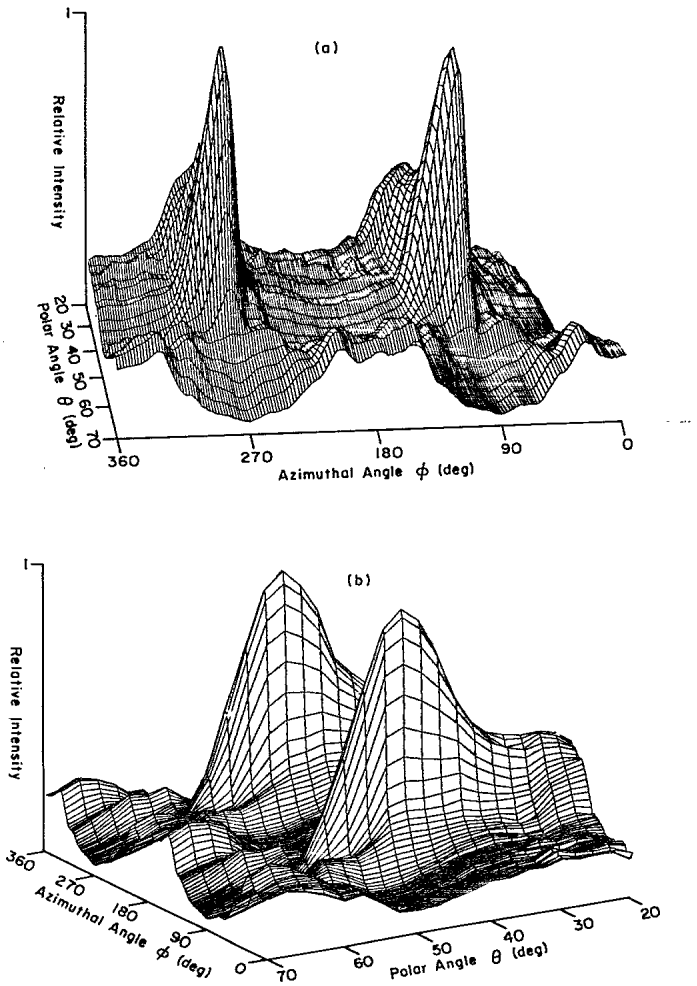

FIG. 5. The relative intensity of 20-eV Ga^+ ions desorbed by 3-keV normal incident Ar^+-ion bombardment of the GaAs{001}-(2×4) surface. The polar angle is the angle of detection from the surface normal. For the in-plane azimuthal angle, $\phi=0°$ corresponds to the ⟨011⟩ crystal direction. (a) Front view and (b) side view.

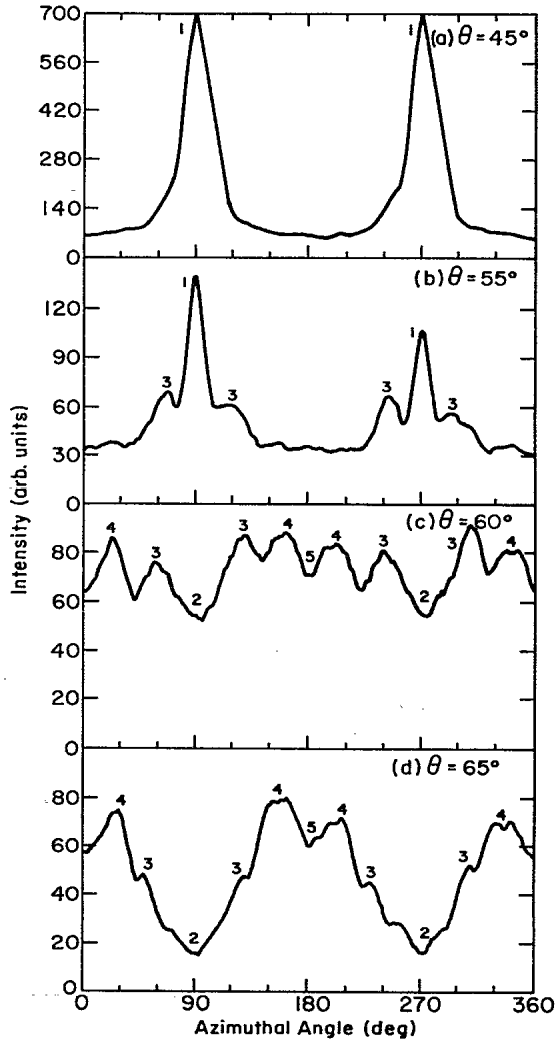

FIG. 6. The absolute intensity of 20-eV Ga^+ ions desorbed from the GaAs{001}-(2×4) surface as a function of azimuthal angle at a polar angle of (a) 45°, (b) 55°, (c) 60°, and (d) 65° from the surface normal. The numbers above the spectral features correspond to secondary-ion ejection mechanisms described in the text and displayed in Fig. 4.

fying explanation for the origin of the major features of the Ga^+-ion distributions from GaAs{001}. To confirm these ideas and to provide a sound theoretical basis for more quantitative studies, it is really necessary to perform computer simulations of the ion-impact event. Unfortunately, classical dynamics calculations are not yet possible for GaAs because of the lack of a suitable interaction potential function.[7] These functions are, of course, necessary to calculate the trajectories of desorbing atoms. There have been recent calculations for the angular distributions of Si atoms ejected from Si{110} and Si{001}-(2×1) using a many-body potential developed by Tersoff.[7] Moreover, results of these calculations were compared with measurements of the Ga^+-ion distributions from GaAs{110} and surprisingly good agreement was achieved.[9] This agreement is possible since the bulk crystal structures of Si and GaAs are closely related and because the response of a solid to keV-ion bombardment is influenced more strongly by structure than by chemical bonding forces.

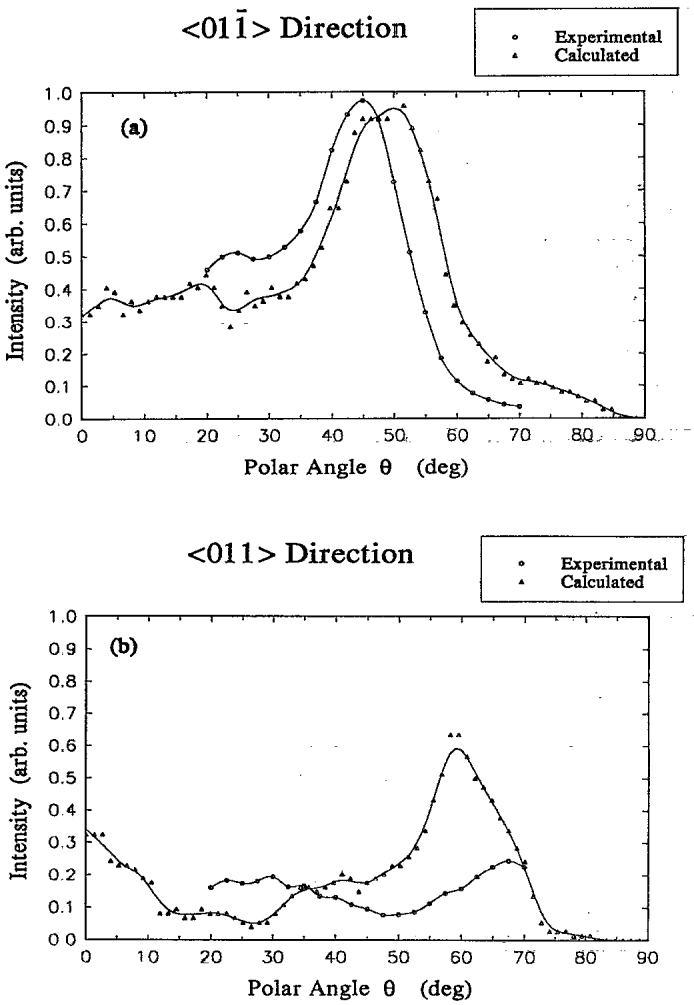

FIG. 7. The experimental and calculated distributions of Ga^+ ions desorbed from the GaAs{001}-(2×4) surface as a function of polar angle from the surface in the (a) ⟨01$\bar{1}$⟩ crystal direction and (b) ⟨011⟩ crystal direction.

Results of these calculations for Si{001}, Si{001}-(2×1), and Si{001}-(2×4) are shown in the bottom part of Fig. 1. All of the computational details associated with these simulations have been discussed previously.[7] These distributions are displayed in a format which allows a real-space comparison to the model crystals of GaAs shown above them. The azimuthal angles are defined relative to the center of each circle as indicated. The polar angle is related to the distance of a spot from the center of the circle. These distributions are for the second-layer Si atoms which are found to eject. This set is crystallographically equivalent to the Ga atoms shown by the shaded atoms of Fig. 1.

In a qualitative sense, the results of these calculations are quite fascinating. For the unreconstructed GaAs{001} surface, the Ga distribution would be expected to exhibit only two peaks, at $\phi=90°$ and 270°, with no structure found at higher polar angles and no intensity at $\phi=0°$ and 180° or $\theta<45°$. These additional features must arise entirely from the reconstruction process. Note also that the (2×1) reconstruction does not yield any intensity along $\phi=0°$ and 180°. As discussed above, this intensity is possible only because of the channel created by the missing row of As_2 dimers found in the (2×4) surface. A detailed analysis of the atomic trajectories leading to these distributions is fully consistent with the simpler, intuitive arguments developed in the preceding section.

It would be valuable to make a more quantitative comparison between our measurements and the calculations. It is dangerous to try to push the model too far because of the obvious assumptions that have been necessary. However, a polar angle plot associated with the calculations is shown in Fig. 1 and the experimental data is shown in Fig. 7. The most important point is that there is quite good agreement between the appropriate results and the relative differences between the $\phi=90°$ and 270° directions and the $\phi=0°$ and 180° directions are accurately predicted. It should be noted that the influence of the image interaction on the Ga^+-ion distribution is uncertain. For GaAs{110} we found that the polar angle plots for Ga^+ ions and Ga neutral atoms were nearly identical, suggesting that this force is rather weak for this system.[9] For GaAs{001}-(2×4), however, the ion originates from a second-layer atom, and the effects may be stronger since the ion may be formed closer to the surface. Moreover, the As-As surface dimer bond distance has not yet been conclusively determined for the GaAs{001}-(2×4) surface. It is not possible to scale the Si{001}-(2×4) simulations to perfectly replicate the GaAs structure without this information, and the polar angle distributions of Fig. 7 should therefore only agree qualitatively between the calculated and experimental curves, as observed.

CONCLUSIONS

We have presented the angular distributions of Ga^+ ions desorbed from a MBE-grown GaAs{001} surface. These distributions are significant for several reasons. (i) A direct atom-atom collisional mechanism causes the ejection of ions along a crystal bond axis. The dominance

of this mechanism in the angular distribution of secondary ions is unique to semiconductor surfaces. (ii) The structure of the GaAs{001}-(2×4) reconstructed surface is such that the detected Ga^+ ions originate almost exclusively from the second atomic layer of the sample. This effect, in conjunction with a direct ejection mechanism, produces angular anisotropies of unprecedented magnitude. (iii) Significant features at high polar angles are associated solely with the reconstruction of the surface. This technique therefore represents a noteworthy approach to examining, in detail, the structure of surfaces. (iv) By combining the analysis of features in the secondary ion angular distributions with RHEED studies, we have confirmed that there are open channels parallel to the $\langle 01\bar{1} \rangle$ direction of the GaAs{001}-(2×4) surface, in accord with previous theoretical and STM studies. We can further conclude that these open channels result from one, and only one, missing As_2 dimer per unit cell. (v) There is an indication, although inconclusive, of possible asymmetry in the angular distributions of secondary ions relative to a plane parallel to the $\langle 011 \rangle$ (or 2×) direction of the surface. This could result from tilting of the As_2 dimers, proposed in several theoretical and experimental studies of this surface. (vi) Secondary ion angular distributions, derived from molecular-dynamics simulations of keV-ion bombardment of the Si{001}-(2×4) surface, are in reasonable qualitative agreement with the experimental distributions from the GaAs{001}-(2×4) surface. The calculated distributions provide insight into the microscopic details of the ion-beam–surface interaction events.

ACKNOWLEDGMENTS

The authors would like to thank Jay Burnham and Steve Goss for their help in performing the experiments. We thank Roger Smith for his contributions to the molecular-dynamics computer simulations. The financial support of the National Science Foundation, the Office of Naval Research, and IBM are gratefully acknowledged. B.J.G. also acknowledges the Camille and Henry Dreyfus Foundation for partial support. The Pennsylvania State University provided the computer time for the simulations.

*Present address: Department of Chemistry, California Institute of Technology, Mail Code 127-72, 218 Noyes, Pasadena, CA 91125.

†Present address: Armament Development Authority (Dept. 23), P.O. Box 2250, Haifa, Israel.

[1]J. H. Neave and B. A. Joyce, J. Cryst. Growth **44**, 387 (1978).

[2]D. L. Miller, Thin Solid Films **118**, 117 (1984).

[3]P. Drathen, W. Ranke, and K. Jacobi, Surf. Sci. **77**, L162 (1978).

[4]M. D. Pashley, K. W. Haberen, W. Friday, J. M. Woodall, and P. D. Kirchner, Phys. Rev. Lett. **60**, 2176 (1988).

[5]D. K. Biegelsen, R. D. Bringans, J. E. Northrup, and L. E. Swartz, Phys. Rev. B **41**, 5701 (1990).

[6]D. E. Harrison, Jr., Crit. Rev. Solid State Mater. Sci. **14**, S1 (1988).

[7]R. Smith, D. E. Harrison, Jr., and B. J. Garrison, Phys. Rev. B **40**, 93 (1989).

[8]N. Winograd, *Desorption Mass Spectrometry* (The American Chemical Society, Washington, D.C., 1985), pp. 83–96.

[9]R. Blumenthal and N. Winograd, Phys. Rev. B **42**, 11 027 (1990).

[10]R. Blumenthal, S. K. Donner, J. L. Herman, R. Trehan, K. P. Caffey, E. Furman, and N. Winograd, J. Vac. Sci. Technol. B **6**, 1444 (1988); R. Blumenthal, thesis, The Pennsylvania State University, 1990.

[11]J. J. Harris, B. A. Joyce, and P. J. Dobson, Surf. Sci. **103**, L90 (1981).

[12]S. P. Holland, B. J. Garrison, and N. Winograd, Phys. Rev. Lett. **43**, 220 (1979).

[13]S. P. Holland, B. J. Garrison, and N. Winograd, Phys. Rev. Lett. **44**, 756 (1980).

[14]B. J. Garrison, N. Winograd, D. M. Deaver, C. T. Reimann, D. Y. Lo, T. A. Tombrello, D. E. Harrison, Jr., and M. H. Shapiro, Phys. Rev. B **37**, 7197 (1988).

[15]K. Caffey, R. Blumenthal, J. Burnham, E. Furman, and N. Winograd, J. Vac. Sci. Technol. B **9**, 2268 (1991).